

Discharge Capacity Fading of $\text{LiCo}_y\text{Mn}_{2-y}\text{O}_4$ with Cycling

IkHyun Kwon and MyoungYoup Song[†]

*Division of Advanced Materials Engineering, Research Center of Advanced Materials Development,
Engineering Research Institute, Chonbuk National University, Jeonju 561-756, Korea*

(Received March 21, 2003; Accepted May 31, 2003)

ABSTRACT

$\text{LiCo}_y\text{Mn}_{2-y}\text{O}_4$ samples were synthesized by calcining a mixture of $\text{LiOH}\cdot\text{H}_2\text{O}$, MnO_2 (CMD) and CoCO_3 calcining at 400°C for 10 h and then calcining twice at 750°C for 24 h in air with intermediate grinding. All the synthesized samples exhibited XRD patterns for the cubic spinel phase with a space group $\text{Fd}\bar{3}\text{m}$. The electrochemical cells were charged and discharged for 30 cycles at a current density $600\ \mu\text{A}/\text{cm}^2$ between 3.5 and 4.3 V. As the value of y increases, the size of particles becomes more homogeneous. The first discharge capacity decreases as the value of y increases, its value for $y=0.00$ being $92.8\ \text{mAh/g}$. The LiMn_2O_4 exhibits much better cycling performance than that reported earlier. The cycling performance increases as the value of y increases. The efficiency of discharge capacity is 98.9% for $y=0.30$. The larger lattice parameter for the smaller value of y is related to the larger discharge capacity. The more quantity of the intercalated and the deintercalated Li in the sample with the larger discharge capacity brings about the larger capacity fading rate.

Key words : $\text{LiCo}_y\text{Mn}_{2-y}\text{O}_4$, Solid-state reaction method, The first discharge capacity, Cycling performance, Capacity fading rate

1. Introduction

The transition metal oxides such as LiCoO_2 ,¹⁻³⁾ LiNiO_2 ,⁴⁻⁶⁾ and LiMn_2O_4 ⁷⁻¹⁵⁾ have been investigated in order to apply them to the cathode materials of lithium secondary battery. LiCoO_2 has large diffusivity and high operating voltage, and it can be easily prepared. However, it contains an expensive element Co. LiNiO_2 has a large discharge capacity¹⁶⁾ and is relatively excellent from the view points of economics and environment. However, its preparation is very difficult as compared with LiCoO_2 and LiMn_2O_4 . LiMn_2O_4 is very cheap and does not bring about environmental pollution, but its cycling performance is not good.

In our previous work,¹³⁾ the variation of the electrochemical properties of LiMn_2O_4 with the calcining temperature was investigated. The LiMn_2O_4 sample calcined at 750°C exhibited a relatively large discharge capacity and a quite good cycling performance.

In this work, in order to improve the cycling performance of LiMn_2O_4 , a part of Mn is replaced by Co in LiMn_2O_4 . $\text{LiCo}_y\text{Mn}_{2-y}\text{O}_4$ samples were prepared by a solid-state reaction method involving calcining at 750°C . Then their electrochemical properties are examined.

2. Experimental

LiMn_2O_4 compound was synthesized by the solid-state reaction method. A mixture of $\text{LiOH}\cdot\text{H}_2\text{O}$ and MnO_2 (CMD) with a 1 : 2 molar ratio were mixed in a mortar filled with ethanol. Excess $\text{LiOH}\cdot\text{H}_2\text{O}$ was added in order to compensate the quantity of evaporated Li during preparation. The mixture was calcined at 400°C for 10 h and then calcined twice at 750°C for 24 h in air with intermediate grinding. The heating rate was $100^\circ\text{C}/\text{h}$ and the cooling rate was $50^\circ\text{C}/\text{h}$. After adding appropriate amounts of CoCO_3 to $\text{LiOH}\cdot\text{H}_2\text{O}$ and MnO_2 , $\text{LiCo}_y\text{Mn}_{2-y}\text{O}_4$ ($y=0.08, 0.15, 0.22, \text{ and } 0.30$) were also synthesized at 750°C by the above same process. The phase identification of the prepared samples was carried out by X-Ray Diffraction (XRD, Rigaku III/A type) analysis using $\text{CuK}\alpha$ radiation. The morphologies of the samples were observed using a Scanning Electron Microscope (SEM). To measure the electrochemical properties, the electrochemical cells consisted of the prepared sample as a positive electrode, Li metal as a negative electrode, and an electrolyte of 1 M LiPF_6 in a 1 : 1 (volume ratio) mixture of Ethylene Carbonate (EC) and Dimethyl Carbonate (DMC). A Whatman glass-fiber was used as a separator. The cells were assembled in an argon-filled dry box. To fabricate the positive electrode, active material, acetylene black, and Polytetrafluoroethylene (PTFE) binder were mixed in a weight ratio 100 : 10 : 1 in an agate mortar. By introducing Li metal, the Whatman glass-fiber, the positive electrode, and the electrolyte, the cell was assembled. All the electrochemical tests were performed at room temperature with a battery charge-discharge cycle tester in a potential range

[†]Corresponding author : MyoungYoup Song

E-mail : songmy@moak.chonbuk.ac.kr

Tel : +82-63-270-2379 Fax : +82-63-270-2386

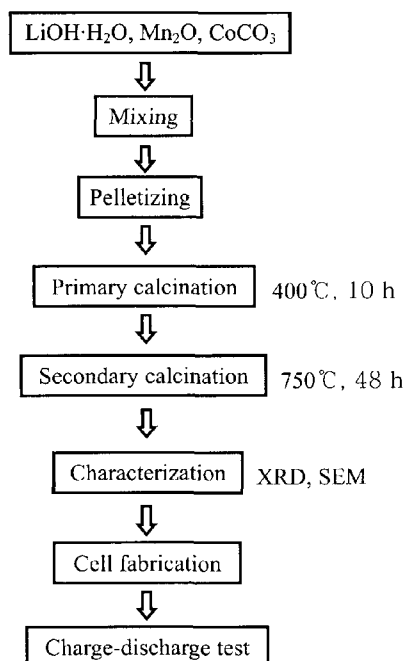


Fig. 1. Schematic diagram of experimental procedure by the solid-state reaction method.

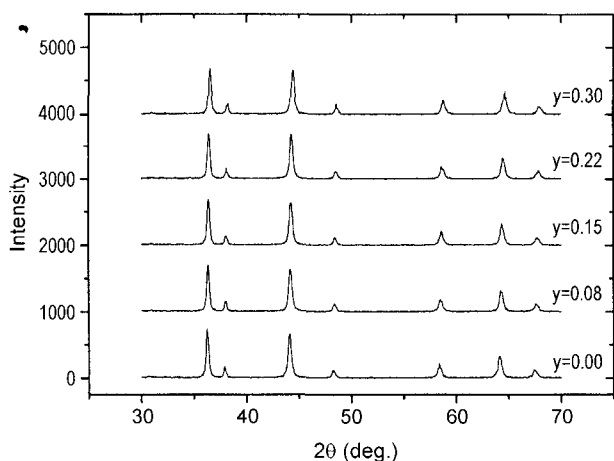


Fig. 2. XRD patterns of $\text{LiCo}_y\text{Mn}_{2-y}\text{O}_4$ synthesized by the solid-state reaction method.

from 3.5 to 4.3 V at a current density $600 \mu\text{A}/\text{cm}^2$. Fig. 1 summarizes the experimental procedure.

3. Results and Discussion

Fig. 2 shows XRD patterns of the $\text{LiCo}_y\text{Mn}_{2-y}\text{O}_4$ ($y=0.00, 0.08, 0.15, 0.22, \text{ and } 0.30$) samples calcined at 750°C for 48 h. All the samples exhibit similar patterns. They were identified as the cubic spinel phase having a space group $\text{Fd}\bar{3}\text{m}$. There is no trend in the sharpness of the peaks, showing that all the samples have similar crystallinities. As the value of y increases, the diffraction angle 2θ of the peaks becomes larger.

The lattice parameter of each sample was obtained by

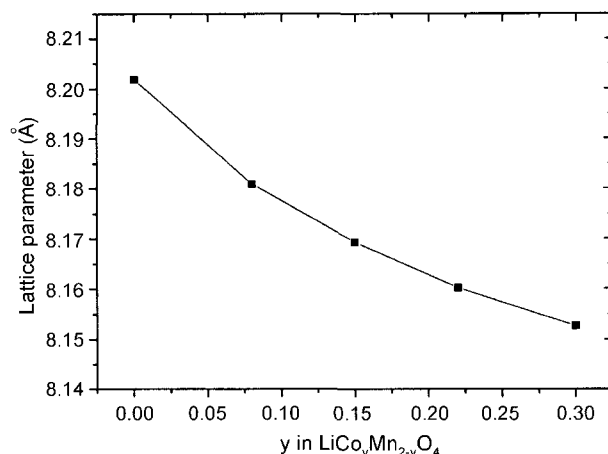


Fig. 3. Variations of the lattice parameter with y in $\text{LiCo}_y\text{Mn}_{2-y}\text{O}_4$ synthesized by the solid-state reaction method.

using the nelson-riley function and the least-squares method and is given in Fig. 3. It decreases as the value of y increases. This is probably because the radius of Co^{3+} is smaller than that of Mn^{3+} . The lattice parameter a (8.201 \AA) for the LiMn_2O_4 is smaller than that (8.237 \AA) reported by Banov *et al.*,¹⁷⁾ who prepared it by a multi-step reaction.

Fig. 4 shows SEM microstructures of the $\text{LiCo}_y\text{Mn}_{2-y}\text{O}_4$ samples. The sample for $y=0.00$ consists of relatively large particles and small particles. The size of the large particles tends to decrease. As the value of y increases, the size of particles becomes more homogeneous. The sample with $y=0.30$ has small particles with relatively homogeneous size.

Fig. 5 shows the variations of the voltage vs. discharge capacity curves in a potential range from 3.5 to 4.3 V at a current density $600 \mu\text{A}/\text{cm}^2$.

All the samples do not show distinct voltage plateaus. As the value of y increases, the voltage plateaus become more ambiguous. The discharge capacities of all the samples decrease as the number of cycle increases. The decreasing rate of discharge capacity according to the number of cycle becomes smaller as the value of y increases. Its value for the samples with $y=0.30$ is extremely small.

Fig. 6 shows the variation of voltage vs. the first discharge capacity curves with the value of y in $\text{LiCo}_y\text{Mn}_{2-y}\text{O}_4$ synthesized by the solid-state reaction method. As the value of y increases, the discharge capacity decreases.

Fig. 7 shows the variations of discharge capacity with the number of cycle for $\text{LiCo}_y\text{Mn}_{2-y}\text{O}_4$ synthesized by the solid-state reaction method. That for LiMn_2O_4 in ref. 12 is also given. The cells were cycled for 30 cycles at a current density $600 \mu\text{A}/\text{cm}^2$ between 3.5 and 4.3 V. The first discharge capacity decreases as the value of y increases, its value for $y=0.00$ being 92.8 mAh/g . The LiMn_2O_4 exhibits much better cycling performance (even at a higher current density) than that reported earlier at a current density $265 \mu\text{A}/\text{cm}^2$.¹³⁾ Excess $\text{LiOH}\cdot\text{H}_2\text{O}$ was added in order to compensate the quantity of the evaporated Li during preparation. The mix-

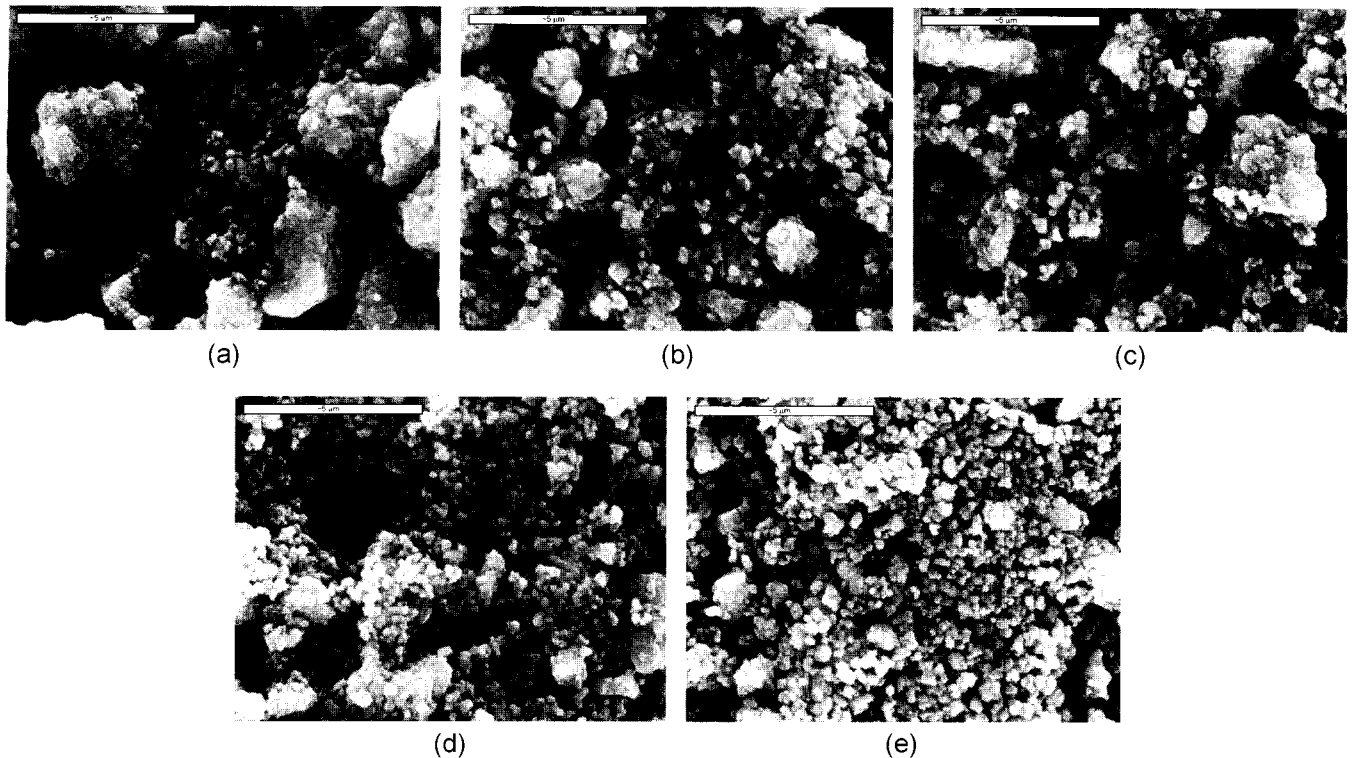


Fig. 4. SEM photographs of $\text{LiCo}_y\text{Mn}_{2-y}\text{O}_4$ (a) $y=0.00$, (b) $y=0.08$, (c) $y=0.15$, (d) $y=0.22$, and (e) $y=0.30$ synthesized by the solid-state reaction method.

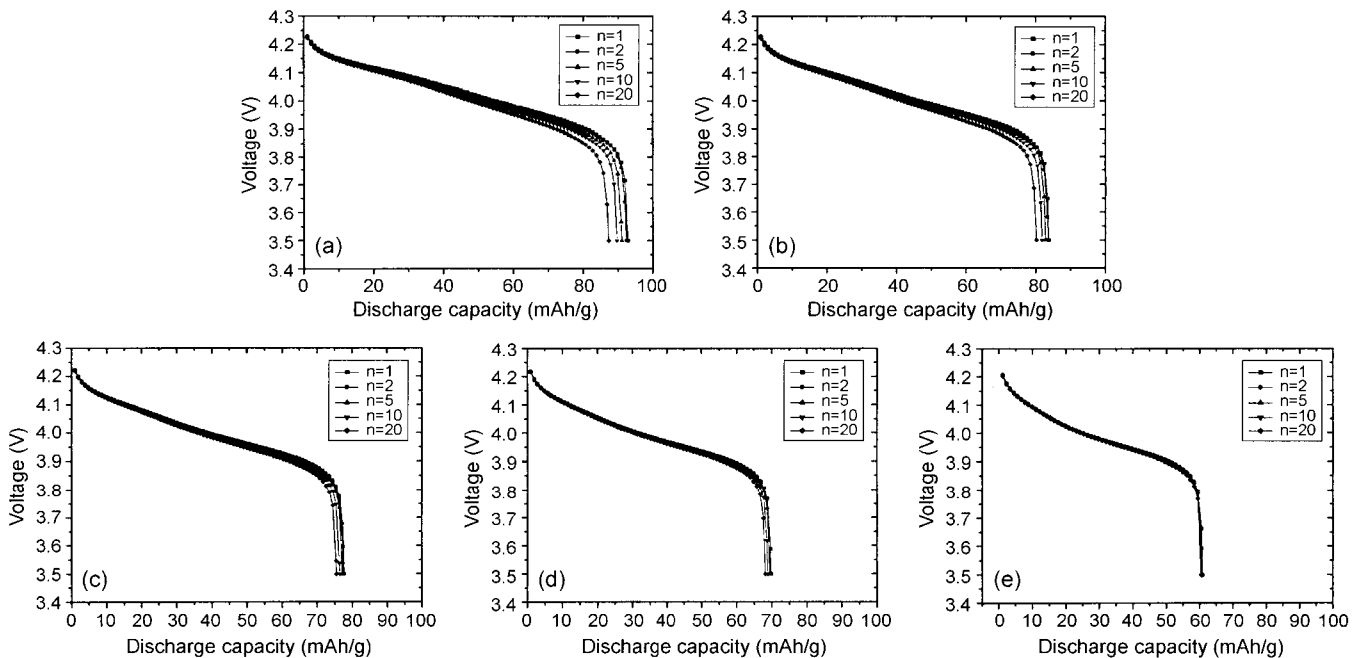


Fig. 5. Variations of voltage vs. discharge capacity curves with the number of cycle for $\text{LiCo}_y\text{Mn}_{2-y}\text{O}_4$ [(a) $y=0.00$, (b) $y=0.08$, (c) $y=0.15$, (d) $y=0.22$, and (e) $y=0.30$] synthesized by the solid-state reaction method.

ture were mixed in a mortar filled with ethanol in order to get a homogeneous mixing. It is considered that these helped the formation of the more LiMn_2O_4 phase per unit weight of sample and the more stable LiMn_2O_4 phase, leading to larger discharge capacities and better performances

than those reported earlier. As the value of y increases, the cycling performance increases. Their efficiencies of discharge capacity are 93.4% for $y=0.00$, 94.8% for $y=0.08$, 96.1% for 0.15, 96.7% for $y=0.22$ and 98.9% for $y=0.30$.

Fig. 8 gives the variations, with y in $\text{LiCo}_y\text{Mn}_{2-y}\text{O}_4$, of lat-

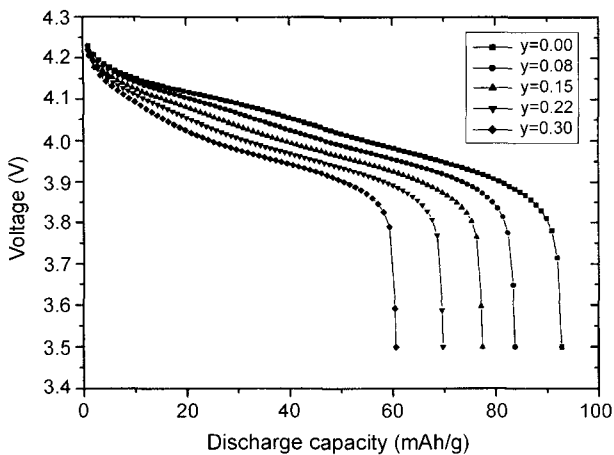


Fig. 6. Variations voltage vs. the first discharge capacity curves with the value y in $\text{LiCo}_y\text{Mn}_{2-y}\text{O}_4$ synthesized by the solid-state reaction method.

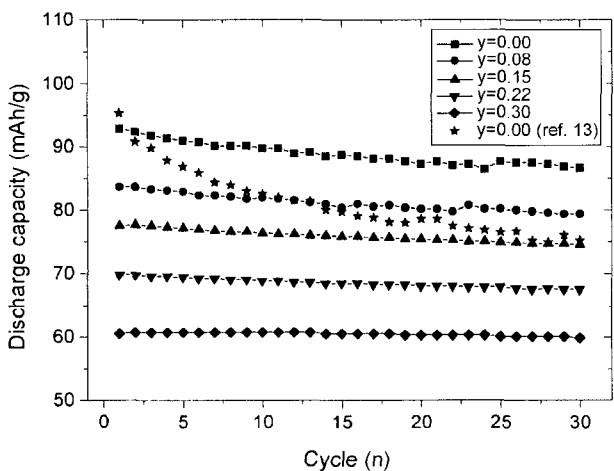


Fig. 7. Variations of discharge capacity with the number of cycle for $\text{LiCo}_y\text{Mn}_{2-y}\text{O}_4$ ($y=0.00, 0.08, 0.15, 0.22, 0.30$) synthesized by the solid-state reaction method.

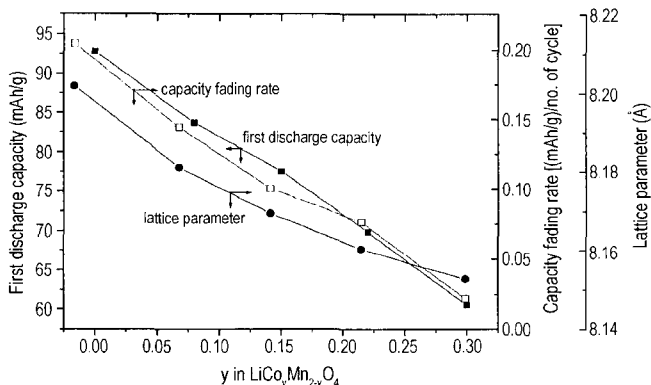


Fig. 8. Variations, with y in $\text{LiCo}_y\text{Mn}_{2-y}\text{O}_4$, of lattice parameter, the first discharge capacity and capacity fading rate.

tice parameter, the first discharge capacity and capacity fading rate. The capacity fading rate, *i.e.* the decrease in the discharge capacity per no. of cycle, is obtained from the first

to the thirtieth cycle. The lattice parameter, the first discharge capacity and the capacity fading rate decrease as the value of y increases. This shows that the sample with a larger lattice parameter has the larger first discharge capacity, suggesting that the spinel structure with a larger lattice parameter intercalates and deintercalates the more Li ions. The larger first discharge capacity is related to the wider range of the value of x in $\text{Li}_x\text{Mn}_2\text{O}_4$. The larger range of the value of x will cause the larger expansion and contraction of the spinel phase LiMn_2O_4 due to the intercalation and deintercalation. This will make the unit cell the more strained and distorted. With cycling, the more interstitial sites and thus the spinel structure will be destroyed. This decreases the larger fraction of the spinel phase, leading to the more capacity fading with cycling.

4. Conclusions

All the synthesized samples exhibited XRD patterns for the cubic spinel phase with a space group $\text{Fd}\bar{3}\text{m}$. The electrochemical cells were charged and discharged for 30 cycles at a current density $600 \mu\text{A}/\text{cm}^2$ between 3.5 and 4.3 V. As the value of y increases, the size of particles becomes more homogeneous. The first discharge capacity decreases as the value of y increases, its value for $y=0.00$ being 92.8 mAh/g. The LiMn_2O_4 exhibits much better cycling performance than that reported earlier. The cycling performance increases as the value of y increases. The efficiency of discharge capacity is 98.9% for $y=0.30$. The larger lattice parameter for the smaller value of y is related to the larger discharge capacity. The more quantity of the intercalated and the deintercalated Li in the sample with the larger discharge capacity brings about the larger capacity fading rate.

Acknowledgement

This work was supported by the Research Center of Advanced Materials Development, Engineering Research Institute at Chonbuk National University.

REFERENCES

1. K. Ozawa, "Lithium-ion Rechargeable Batteries with LiCoO_2 and Carbon Electrodes: The LiCoO_2/C System," *Solid State Ionics*, **69** 212-21 (1994).
2. R. Alcantara, P. Lavela, J. L. Tirado, R. Stoyanova, and E. Zhecheva, "Structure and Electrochemical Properties of Boron-doped LiCoO_2 ," *J. Solid State Chem.*, **134** 265-73 (1997).
3. Z. S. Peng, C. R. Wan, and C. Y. Jiang, "Synthesis by Sol-gel Process and Characterization of LiCoO_2 Cathode Materials," *J. Power Sources*, **72** 215-20 (1998).
4. J. M. Tarascon, E. Wang, F. K. Shokoohi, W. R. McKinnon, and S. Colson, "The Spinel Phase of LiMn_2O_4 as a Cathode in Secondary Lithium Cells," *J. Electrochem. Soc.*, **138** 2859-64 (1991).
5. M. Y. Song and R. Lee, "Synthesis by Sol-gel Method and

- Electrochemical Properties of LiNiO_2 Cathode Material for Lithium Secondary Battery," *J. Power Sources*, **111** 97-103 (2002).
6. H. Rim, S. G. Kang, S. H. Chang, and M. Y. Song, "A Study on the Synthesis and the Electrochemical Properties of $\text{LiNi}_{1-y}\text{Co}_y\text{O}_2$ from Li_2CO_3 , NiCO_3 , and CoCO_3 ," *J. Kor. Ceram. Soc.*, **38** [6] 515-21 (2001).
 7. M. Y. Song, R. Lee, and I. H. Kwon, "Synthesis by Sol-gel Method and Electrochemical Properties of $\text{LiNi}_{1-y}\text{Al}_y\text{O}_2$ Cathode Materials for Lithium Secondary Battery," *Solid State Ionics*, **156** [3-4] 319-28 (2003).
 8. M. Y. Song, H. Rim, E. Y. Bang, S. G. Kang, and S. H. Chang, "Synthesis of Cathode Materials $\text{LiNi}_{1-y}\text{Co}_y\text{O}_2$ from Various Starting Materials and their Electrochemical Properties," *J. Kor. Ceram. Soc.*, **40** [6] 507-12 (2003).
 9. J. R. Dahn, U. von Sacken, and C. A. Michal, "Structure and Electrochemistry of $\text{Li}_{1+y}\text{NiO}_2$ and a New Li_2NiO_2 Phase with the $\text{Ni}(\text{OH})_2$ Structure," *Solid State Ionics*, **44** 87-97 (1990).
 10. J. R. Dahn, U. von Sacken, M. W. Juzkow, and H. Al-Janaby, "Rechargeable $\text{LiNiO}_2/\text{Carbon}$ Cells," *J. Electrochem. Soc.*, **138** 2207-12 (1991).
 11. A. Marini, V. Massarotti, V. Berbenni, D. Capsoni, R. Riccardi, E. Antolini, and B. Passalacqua, "On the Thermal Stability and Defect Structure of the Solid Solution $\text{Li}_x\text{Ni}_{1-x}\text{O}_2$," *Solid State Ionics*, **45** 143-55 (1991).
 12. W. Ebner, D. Fouchard, and L. Xie, "The $\text{LiNiO}_2/\text{Carbon}$ Lithium-ion Battery," *Solid State Ionics*, **69** 238-56 (1994).
 13. M. Y. Song and D. S. Ahn, "On the Capacity Deterioration of Spinel Phase LiMn_2O_4 with Cycling around 4 V," *Solid State Ionics*, **112** 21-2 (1998).
 14. M. Y. Song, D. S. Ahn, and H. R. Park, "Capacity Fading of Spinel Phase LiMn_2O_4 with Cycling," *J. Power Sources*, **83** 57-60 (1999).
 15. D. S. Ahn and M. Y. Song, "Variations of the Electrochemical Properties of LiMn_2O_4 with Synthesis Conditions," *J. Electrochem. Soc.*, **147** [3] 874-79 (2000).
 16. M. Y. Song and M. S. Shon, "Variations of the Electrochemical Properties of LiMn_2O_4 with the Calcining Temperature," *J. Kor. Ceram. Soc.*, **39** [6] 523-27 (2002).
 17. M. Y. Song, I. H. Kwon, and M. S. Shon, "Electrochemical Properties of $\text{LiNi}_y\text{Mn}_{2-y}\text{O}_4$ Prepared by the Solid-state Reaction," *J. Kor. Ceram. Soc.*, **40** [5] 401-04 (2003).
 18. I. H. Kwon and M. Y. Song, "Electrochemical Properties of $\text{LiCo}_y\text{Mn}_{2-y}\text{O}_4$ Synthesized by the Combustion Method for Lithium Secondary Battery," *Solid State Ionics*, **158** [1-2] 103-11 (2003).
 19. Y. Nishida, K. Nakane, and T. Stoh, "Synthesis and Properties of Gallium-doped LiNiO_2 as the Cathode Material for Lithium Secondary Batteries," *J. Power Sources*, **68** 561-64 (1997).
 20. B. Banov, Y. Todorov, A. Trifonova, A. Momchilov, and V. Manev, " $\text{LiMn}_{2-x}\text{Co}_x\text{O}_4$ Cathode with Enhanced Cycleability," *J. Power Sources*, **68** 578-81 (1997).